

# A coupled discrete/continuous method for computing lattices. Application to a masonry-like structure

Mohammad Hammoud\*, Karam Sab, Denis Duhamel

Université Paris-Est, UR Navier, Ecole des Ponts ParisTech, 6 et 8 Avenue Blaise Pascal, Cité Descartes, Champs sur Marne, 77455 Marne La Vallée, Cedex 2, France

## ARTICLE INFO

### Article history:

Received 8 July 2010

Received in revised form 30 June 2011

Available online 20 July 2011

### Keywords:

Discrete  
Finite element  
Homogenization  
Masonry  
Interface  
Coupling

## ABSTRACT

This paper presents a coupled discrete/continuous method for computing lattices and its application to a masonry-like structure. This method was proposed and validated in the case of a one dimensional (1D) railway track example presented in Hammoud et al. (2010). We study here a 2D model which consists of a regular lattice of square rigid grains interacting by their elastic interfaces in order to prove the feasibility and the robustness of our coupled method and highlight its advantages. Two models have been developed, a discrete one and a continuous one. In the discrete model, the grains which form the lattice are considered as rigid bodies connected by elastic interfaces (elastic thin joints). In other words, the lattice is seen as a “skeleton” in which the interactions between the rigid grains are represented by forces and moments which depend on their relative displacements and rotations. The continuous model is based on the homogenization of the discrete model (Cecchi and Sab, 2009). Considering the case of singularities within the lattice (a crack for example), we develop a coupled model which uses the discrete model in singular zones (zones where the discrete model cannot be homogenized), and the continuous model elsewhere. A new criterion of coupling is developed and applied at the interface between the discrete and the continuum zones. It verifies the convergence of the coupled solution to the discrete one and limits the size of the discrete zone. A good agreement between the full discrete model and the coupled one is obtained. By using the coupled model, an important reduction in the number of degrees of freedom and in the computation time compared to that needed for the discrete approach, is observed.

© 2011 Elsevier Ltd. All rights reserved.

## 1. Introduction

The aim of this paper is to propose an extension to 2D structures of the 1D coupled method between discrete and continuum media proposed in Hammoud et al. (2010). We focus here on the robustness and the feasibility of the coupled method in the presence of cracks and stress concentrations.

Actually, the 1D model studied in Hammoud et al. (2010) consisted of a beam resting on an elastic springs. The deflection of the beam (as well as the nodal parameters) was calculated by using two approaches; a discrete approach and a macroscopic approach deduced from the discrete one. A comparison between the response of the system obtained by using these approaches showed the cases where the macroscopic approach cannot replace the discrete one. This difference led us to apply a discrete/continuum coupling method. A new criterion of coupling was developed and applied at the interface of the discrete and continuum sub-

domains. In the coupled approach, the macroscopic scale was the initial scale computation. A local discrete computation was done on each macroscopic element. A comparison was done between the nodal parameters computed by the local discrete method and the continuum one. If a strong difference was observed, a refinement of the computation scale was done. This procedure of refinement was necessary in the zone of singularities.

In this present research, a 2D model will be considered. A masonry panel can be described by a discrete model or a continuous model. See Alpa and Monetto (1994), Sab (1996), Cecchi and Sab (2004), Cecchi and Sab (2004) and Cluni and Gusella (2004), for example. In the discrete model, the blocks which form the masonry wall are modeled as rigid bodies connected by elastic interfaces. Then, the masonry is seen as “skeleton” in which the interactions between the rigid blocks are represented by forces and moments which depend on their relative displacements and rotations. The second model is a continuous one based on the homogenization of the discrete model. The aim of this paper is to extend the 1D coupled method of Hammoud et al. (2010) to 2D structures in the presence of cracks and stress concentrations.

Many coupled approaches between discrete and continuum media were developed. See among others the works of Broughton et al. (1999), Curtin and Miller (2003), Wagner and Liu (2003),

\* Corresponding author. Address: Institut Pprime, ENSMA, France. Tel.: +33 5 49 49 82 26.

E-mail addresses: [hammoudm@ensma.fr](mailto:hammoudm@ensma.fr), [mouhamad.hammoud@gmail.com](mailto:mouhamad.hammoud@gmail.com) (M. Hammoud), [sab@enpc.fr](mailto:sab@enpc.fr) (K. Sab), [duhamel@enpc.fr](mailto:duhamel@enpc.fr) (D. Duhamel).

Fish and Chen (2004), Xiao and Belytschko (2004), Ricci et al. (2005), Klein and Zimmerman (2006), Rousseau et al. (2008) and Rousseau et al. (2009). In these works, the domain is decomposed into sub-domains; discrete, continuum and an interface between the discrete and continuum sub-domains. A handshake zone where the two descriptions of material figure can exist at the interface sub-domain. These approaches are divided into energy-based or force-based formulations. Briefly, in the energy-based formulation, it is assumed that the total energy of a domain can be written as the sum of the energy of the three sub-domains discrete, continuum and handshake from which it is composed. The energy of the handshake region is a partition-of-unity blending of discrete and continuum energy descriptions. For example, a well-known energy-based method which includes a handshake region is the bridging domain (BD) method described in Xiao and Belytschko (2004). Within the BD handshake region, both the continuum and discrete energies are used, but their contributions are weighted according to a function  $\theta$  that varies linearly from 1 at the edge of the handshake region closest to the continuum one to 0 at the edge closest to the discrete zone. The total energy is then minimized subject to the imposed displacement boundary conditions to obtain the equilibrium configuration of the system. The approximation inherent to an energy-based coupling of this type leads to errors known as “ghost forces”. The ghost forces are defined as follows: Consider a model in which the discrete elements are on their equilibrium state, and the finite elements are unstressed and undeformed. Physically, this should be an equilibrium configuration where all forces are zero, and therefore any residual forces on the discrete element or nodes that arise in this configuration are unphysical and will lead to spurious distortions of the domain upon relaxation. These unphysical forces are the ghost forces. The existence of ghost forces is, it seems, a necessary consequence of having well-defined energy functional. All energy-based methods mentioned above, suffer from these forces in various degrees. An alternate approach is to abandon the energy-based approach and instead starts from the forces directly. Methods of this type can indeed eliminate the ghost forces (see Kohlhoff et al., 1991). In these approaches, there is no handshake zone and strong compatibility sets the position of the discrete element and the nodes along the interface zone. A force-based method is based on the following philosophy: to eliminate ghost forces, design the method so that the forces are identically zero when the perfect discrete sub-domain is in its correct equilibrium state. Since it does not seem possible to do this in general using an energy functional, we derive forces without recourse to a total energy. For more details, an exhaustive literature review of these coupled models has been given in Hammoud et al. (2010).

In the energy-based and the force-based formulations, the size of the discrete zone is not defined. It depends on many parameters as the weight function, the boundary conditions at the interface zone, etc. In our force-based formulation, there is no handshake zone and the discrete zone that contains the singularities is fixed at the beginning of the simulation. It will be controlled by a special coupling criterion at the interface zone, described in (Section 4.2.2). If the value of this criterion is not small enough to ensure a convergence, the size of the discrete zone will be increased. This iterative procedure is repeated until convergence of the coupled solution to the discrete one is reached.

As for the 1D model (Hammoud et al., 2010), the mechanical parameters of the system being studied will be calculated in a way that does not require the calculation of the energy and avoids the problem of how to partition this energy between the discrete and continuum zones at the interface. We will calculate the global rigidity matrices (discrete ( $\mathbf{K}^D$ ), continuous ( $\mathbf{K}^C$ ) and interaction ( $\mathbf{K}^{C-D}$ )) and then solve a linear system written as follows:

$$\underbrace{\begin{pmatrix} \mathbf{K}^C & 0 \\ 0 & \mathbf{K}^D \end{pmatrix} + \mathbf{K}^{C-D}}_{\mathbf{K}^{\text{total}}} \begin{pmatrix} \mathbf{U}^C \\ \mathbf{U}^D \end{pmatrix} = \mathbf{F}^{\text{total}}. \quad (1)$$

In this present research, at first, we present the 2D masonry model. Secondly, we develop the discrete and the continuous models used to calculate the behavior of the masonry panel. The continuous boundary value problem is solved by using the Finite Element Method. We implement the full continuous and the full discrete models in a MATLAB code as well as the coupled discrete/continuous one. This case is validated in comparison with a FE software (ABAQUS). We also develop a numerical bench test in order to prove that the discrete medium is homogenizable in the case of no singularities. In the case where singularities exist in the structure (a crack for example), a criterion of coupling between discrete and continuous models, is developed. Near the crack, a discrete zone is used and farther a FE mesh is employed. The criterion of coupling applied at the interface of these zones, verify the convergence of the coupled solution to that discrete. The size of the discrete zone is limited and a considerable reduction of the DoFs is also observed.

## 2. The discrete model

The 2D model consists of a regular lattice of square rigid grains interacting by their elastic interfaces (see Fig. 1).

The in-plane motion of the grain can be described by two displacements and one rotation at the center.

The geometry of the lattice is described hereafter. The position of the center of grain  $B^{ij}$ ,  $\mathbf{y}^{ij}$ , in the Euclidean space is formulated as follows:

$$\mathbf{y}^{ij} = ia\mathbf{e}_1 + ja\mathbf{e}_2, \quad (2)$$

$\mathbf{e}_1, \mathbf{e}_2, \mathbf{e}_3$  is an orthonormal base.

So the displacement of the  $B^{ij}$  grain is an in plane rigid body motion:

$$\mathbf{u}(\mathbf{y}) = \mathbf{u}^{ij} + \boldsymbol{\omega}^{ij} \times (\mathbf{y} - \mathbf{y}^{ij}), \quad \forall \mathbf{y} \in B^{ij} \quad (3)$$

where

$$\mathbf{u}^{ij} = u_1^{ij}\mathbf{e}_1 + u_2^{ij}\mathbf{e}_2 \quad \text{and} \quad \boldsymbol{\omega}^{ij} = \omega_3^{ij}\mathbf{e}_3. \quad (4)$$

If the mortar joint is modeled as an elastic interface, then the constitutive law is a linear relation between the tractions on the block surfaces and the jump of the displacement:

$$\mathbf{t} = \boldsymbol{\sigma} \mathbf{n} = \mathbf{K} \cdot \mathbf{d} \quad \text{on } S. \quad (5)$$

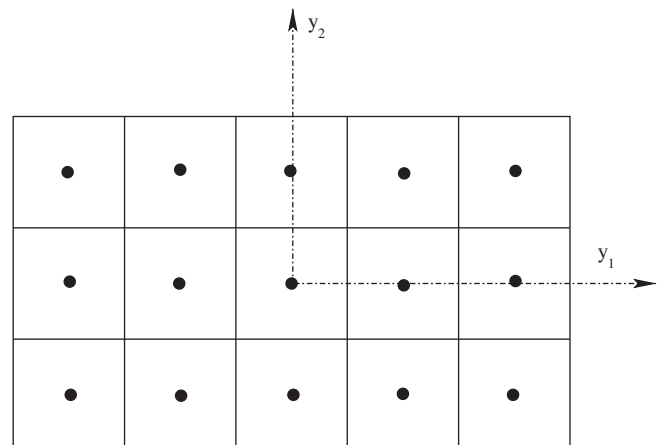


Fig. 1. Square grains forming the regular lattice.

Here,  $\sigma$  is the stress tensor,  $\mathbf{n}$  is the normal to the interface  $S$  and  $\mathbf{d}$  is the displacement jump at  $S$ . For isotropic mortar, the elastic interface stiffness tensor  $\mathbf{K}$  is given as:

$$\mathbf{K} = \frac{1}{e} (\mu^M \mathbf{I} + (\lambda^M + \mu^M) (\mathbf{n} \otimes \mathbf{n})), \quad (6)$$

where  $\lambda^M$  and  $\mu^M$  are the Lamé constants of the mortar and  $e$  is the thickness of the real joint.

The elastic strain energy associated to the interface  $S$  is:

$$\mathcal{W} = \frac{1}{2} \int_S \mathbf{d} \cdot (\mathbf{K} \cdot \mathbf{d}) dS \quad (7)$$

Note that each grain has four neighbours that mean four interfaces in which two are horizontal and two are vertical, as shown in Fig. 2. The vectors  $\mathbf{C}^+ \mathbf{M}_1$  and  $\mathbf{C}^- \mathbf{M}_1$  are given by:

$$\mathbf{C}^+ \mathbf{M}_1 = -\frac{a}{2} \mathbf{e}_1 + y \mathbf{e}_2, \quad (8)$$

$$\mathbf{C}^- \mathbf{M}_1 = \frac{a}{2} \mathbf{e}_1 + y \mathbf{e}_2.$$

So the displacement of a point located on the vertical interface is written as follows:

$$\begin{aligned} \mathbf{u}^+(M_1) &= \mathbf{u}(C^+) + \omega^+ \times \mathbf{C}^+ \mathbf{M}_1, \\ \mathbf{u}^-(M_1) &= \mathbf{u}(C^-) + \omega^- \times \mathbf{C}^- \mathbf{M}_1. \end{aligned} \quad (9)$$

Thus, the displacement jump at  $S$  can be written as:

$$\begin{aligned} \mathbf{d} &= \mathbf{u}^+(M_1) - \mathbf{u}^-(M_1) = d_1 \mathbf{e}_1 + d_2 \mathbf{e}_2 \\ &= (u^+ - u^- + (\omega^- - \omega^+) y) \mathbf{e}_1 \\ &\quad + \left( v^+ - v^- - (\omega^- + \omega^+) \frac{a}{2} \right) \mathbf{e}_2. \end{aligned} \quad (10)$$

Let  $U$  be the vector of displacement and rotation of two neighbouring grains:  $U = [u^+ \ v^+ \ \omega^+ \ u^- \ v^- \ \omega^-]^T$ . Then, the elastic strain energy associated to the vertical interface takes the following form:

$$\mathcal{W} = \frac{1}{2} U^T \mathcal{K}_{\text{vertical}} U. \quad (11)$$

By using the relationship (7), the value of the elastic strain energy is calculated. So, from (11), we extract the form of the vertical stiffness tensor of the vertical interface ( $\mathcal{K}_{\text{vertical}}$ ) as follows:

$$\begin{pmatrix} \frac{K''a}{e^v} & 0 & 0 & -\frac{K'a}{e^v} & 0 & 0 \\ 0 & \frac{K''a}{e^v} & -\frac{K''a\sqrt{2}}{4e^v} & 0 & -\frac{K''a}{e^v} & -\frac{K''a\sqrt{2}}{4e^v} \\ 0 & -\frac{K''a\sqrt{2}}{4e^v} & \frac{(K'+3K'')a}{24e^v} & 0 & \frac{K''a\sqrt{2}}{4e^v} & \frac{(-K'+3K'')a}{24e^v} \\ -\frac{K'a}{e^v} & 0 & 0 & \frac{K'a}{e^v} & 0 & 0 \\ 0 & -\frac{K''a}{e^v} & \frac{K''a\sqrt{2}}{4e^v} & 0 & \frac{K''a}{e^v} & \frac{K''a\sqrt{2}}{4e^v} \\ 0 & -\frac{K''a\sqrt{2}}{4e^v} & \frac{(-K'+3K'')a}{24e^v} & 0 & \frac{K''a\sqrt{2}}{4e^v} & \frac{(K'+3K'')a}{24e^v} \end{pmatrix}, \quad (12)$$

where  $K'' = \lambda^M + 2\mu^M$ ,  $K' = \mu^M$  and  $e^v$  is the thickness of the vertical joint between two grains.

Similarly, the form of the horizontal stiffness tensor of the horizontal interface  $\mathcal{K}_{\text{horizontal}}$  can be found. It will be used to calculate the global stiffness matrix of the domain.

Hence, the vector of all in-plane degrees of freedom of the structure is calculated by solving the following linear system:

$$\mathbb{K} \mathbb{U} = \mathbb{F} \quad (13)$$

in which  $\mathbb{U} = [u_1 \ v_1 \ \omega_1 \ \dots \ u_N \ v_N \ \omega_N]^T$  is the vector of all in-plane degrees of freedom of the structure under consideration and  $\mathbb{F} = [f_1 \ t_1 \ m_1 \ \dots \ f_N \ t_N \ m_N]^T$  is the vector of all in-plane elastic actions.  $\mathbb{K}$  is the in-plane stiffness matrix calculated by assembling the vertical and horizontal interfaces matrices of the structure.

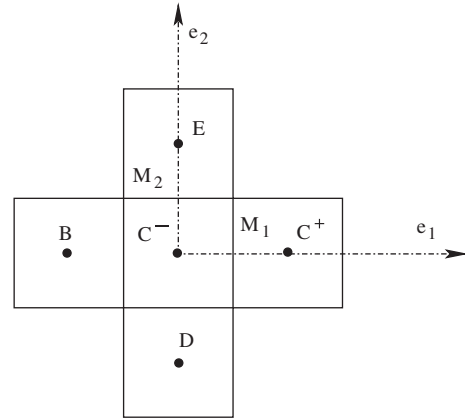


Fig. 2. Horizontal and vertical interfaces of a grain.

### 3. The continuum model

The homogenization of periodic discrete materials has been previously presented in Sab (1996), Pradel and Sab (1998a), Pradel and Sab (1998b), Cecchi and Sab (2002a) and Florence and Sab (2006), for example. The geometry will be discretized by using the Finite Element Method. As mentioned above, the implementation of the homogenized model will be done with a Matlab code in order to couple later, a continuum zone to a discrete one.

Let us consider the static case of the elastic behavior of the domain. The equilibrium equation is written as:

$$\nabla \cdot \sigma + \mathbf{b} = 0, \quad (14)$$

where  $\nabla$  is the divergence operator,  $\sigma$  is the Cauchy stress tensor and  $\mathbf{b}$  the external load applied on the domain. The stress-strain relationship is given by:

$$\sigma = \mathbb{A} : \epsilon, \quad (15)$$

where  $\mathbb{A}$  is the homogenized elastic tensor and  $\epsilon$  is the strain tensor.

Using a weak variational formulation, the equilibrium Eq. (14) is written as follows:

$$\mathbb{K} \mathbb{U} = \mathbb{F}, \quad (16)$$

where  $\mathbb{K}$  is the global stiffness matrix of the domain,  $\mathbb{U}$  is the global vector of nodal displacements and  $\mathbb{F}$  is the global vector of external forces applied on the finite element nodes.

In other words,  $\mathbb{K}$  and  $\mathbb{F}$  are the assembling of the elementary stiffness matrix  $\mathbb{K}^e$  and the force vector  $\mathbb{F}^e$ , respectively.

$\mathbb{A}$  is the homogenized elastic tensor. It is written as follows:

$$\mathbb{A} = \begin{bmatrix} A_{1111}^{\text{hom}} & 0 & 0 \\ 0 & A_{2222}^{\text{hom}} & 0 \\ 0 & 0 & A_{1212}^{\text{hom}} \end{bmatrix}, \quad (17)$$

where  $A_{1111}^{\text{hom}} = \frac{K'a}{e^h}$ ,  $A_{2222}^{\text{hom}} = \frac{K''a}{e^h}$  and  $A_{1212}^{\text{hom}} = \frac{2K''a}{e^h}$ .  $K' = \lambda^M + 2\mu^M$ ,  $K'' = \mu^M$  and  $e^h$  is the thickness of the joint between two grains.

### 4. Numerical simulations

#### 4.1. Discrete model versus continuous model

##### 4.1.1. Compression test

Let us consider a panel (width  $L$  and height  $H$ ) subjected to compression actions  $F$  (see Table 1), supported at its left and right edges with  $u_2(X=0, X=L) = 0$ , fixed at the base  $u_1(Y=0) =$

**Table 1**  
Mechanical parameters for numerical simulations.

	$E$	$\nu$	$e^D = e^h$	$F$	$L$	$H$
Values	1000 MPa	0.3	0.2 mm	1N	4 m	4 m

$u_1(Y = 0) = \omega_3 = 0$  and loaded with a vertical uniform force applied on the upper edge (see Fig. 3).

In the discrete model, the uniform load is applied on each grain center of the upper edge. In the continuous one, the load is applied at the nodes of the finite element. The DE dimensions are (16cm × 16cm) and the FE dimensions are (64cm × 32cm). In Fig. 4, the nodal displacements of the middle line of the panel ( $Y = \frac{H}{2}$ ),  $u_2$ , are represented. We observe a good match between the discrete and continuous displacements. This matching means that the discrete medium is homogeneizable and the continuous model can replace correctly the discrete one.

**4.1.2. Shear test**

The case of shear stress is investigated in this part. In the discrete model, the panel is under the following boundary conditions:

- grains at the top of the panel: uniform horizontal force,
- grains in the left side of the panel  $u_2 = 0$  and  $u_1, \omega_3$  are free,
- grains in the right side of the panel  $u_2 = 0$  and  $u_1, \omega_3$  are free,
- blocks at the base of the panel  $u_1 = u_2 = 0$  and  $\omega_3$  is free.

In the continuous model, the boundary conditions are the following:  $u_2(x_1 = 0) = u_2(x_1 = L) = 0$ ,  $u_1(x_1 = 0) = u_2(x_1 = 0) = 0$  and a horizontal uniform load is applied at the side  $x_2 = H$  (see Fig. 5).

By considering the discrete medium at coarse scale (the size of a DE is the double of a FE one) and the continuous model at fine scale, it is obtained that the  $u_1$  displacements of the middle line of the panel do not match correctly and the relative difference is more than 10% (Fig. 6). If we refine the coarse scale of the discrete medium (the size of a DE is half of a FE one), this difference will be negligible as we can observe on the (Fig. 6).

Finally, we conclude that the discrete solution converges to the continuous one when the computation scale is fine. This convergence also means, that the discrete medium is homogeneizable and the continuous model can replace correctly the discrete one when there is no singularities in the structure.

It is clear that the computation time and the number of degrees of freedom (DOFs) in the discrete model are more important than that of the continuous model. In what follows, in the case of the shear test studied above, a simple comparison (Table 2) shows the importance of these two factors: computation time and gain in DOFs.

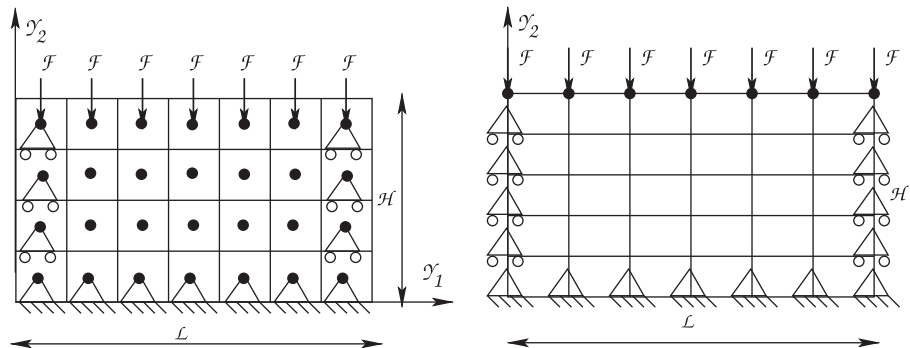


**Fig. 3.** Masonry panel (width  $L$  and height  $H$ ) subject to compression actions supported at its left and right edges  $u_2 = 0$ , fixed at the base loaded with a vertical uniform force applied on the upper edge: (a) discrete model, (b) continuous model.

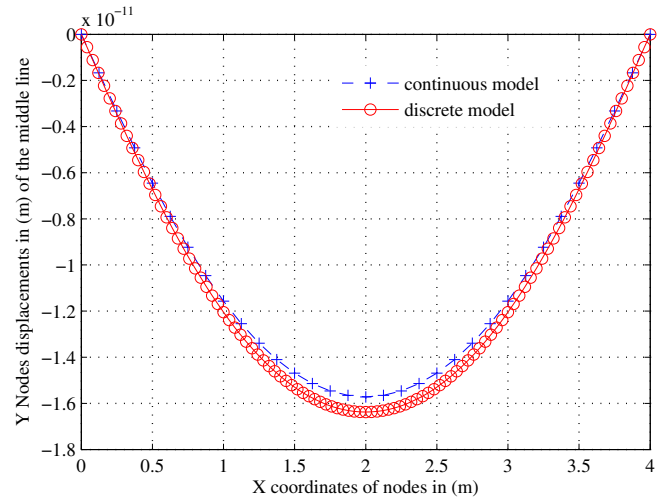


**Fig. 4.** Comparison between discrete and continuous displacements of the nodal line ( $Y = H/2$ ); compression test.

**4.2. The coupling model**

Now we consider a crack in the panel. Near this crack the medium cannot be homogenized. It is noted that the discrete model can be used to simulate all the medium, but taking into account the computation time and the number of DoFs, it will be better if we can couple the continuous and discrete models, then the discrete model is used in the cracked zone and the continuous one is used elsewhere.

**4.2.1. Principle of the coupling model**

The medium is decomposed into two regions. The first one is the continuum region modeled by finite elements (rectangular with two DoFs by node), the second is the discrete region where the Discrete Element (DE) are the centre of grains (3 DoFs at the center of grains). At the interface between these zones, interpolated DE are used to link the FE of the continuum zone to the DE of the discrete zone (see Fig. 7).

As mentioned before, by noting  $E^D$  the elastic energy of the discrete zone,  $E^C$  the elastic energy of the continuum one and  $E^{C-D}$  the energy of interaction between the DEs and the FEs at the interface, the total energy of the coupled medium is given by:

$$E^{\text{total}} = E^D + E^C + E^{C-D} \tag{18}$$

The interaction energy between two DEs ( $-$  and  $+$ ) (see Fig. 8) is written as follows:

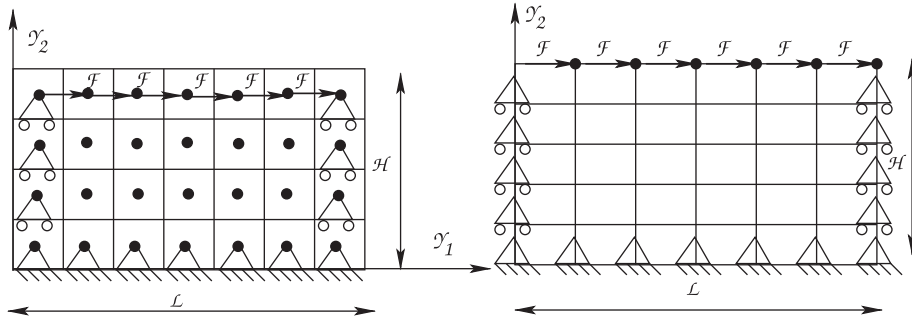


**Fig. 5.** Masonry panel (width  $L$  and height  $H$ ) subject to shear actions simply supported at its left and right edge  $u_2 = 0$  and fixed at the base loaded with a horizontal uniform force applied on the top: (a) discrete model, (b) continuous model.

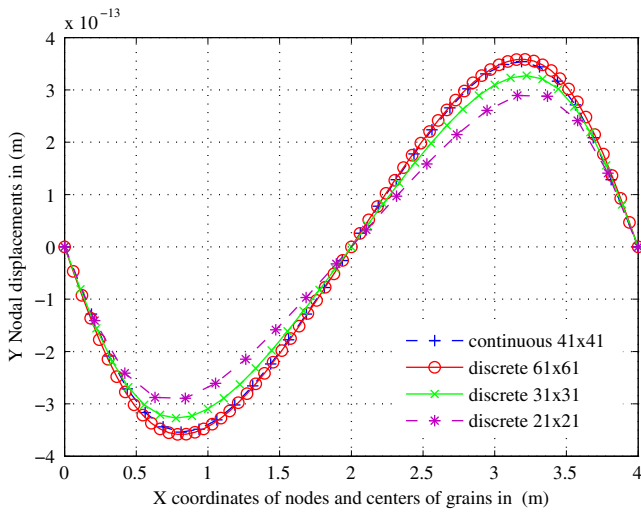


**Fig. 6.** Comparison between discrete and continuous displacements of the middle line ( $Y = H/2$ ); shear test.

$$\mathbf{E}^I = \frac{1}{2} \begin{pmatrix} \mathbf{U}^- \\ \mathbf{U}^+ \end{pmatrix}^T [\mathbf{K}^I] \begin{pmatrix} \mathbf{U}^- \\ \mathbf{U}^+ \end{pmatrix}, \quad (19)$$

$\mathbf{E}^I$  and  $\mathbf{K}^I$  are the interaction energy and the stiffness matrix of the interface between two adjacent grains, respectively.  $\mathbf{U}^-$  and  $\mathbf{U}^+$  are the vectors of displacements and rotation of the grains (-) and (+), respectively.

If we consider a FE modeled by DEs, a relationship between the displacement of the FE node's ( $\square$ ) and the displacement of the DE ( $\circ$  created inside the FE) can be established by interpolation, using the shape functions. By noting  $[U, V, W]^T$  the vector of displacements and rotation of a DE and  $[u_1, v_1, u_2, v_2, u_3, v_3, u_4, v_4]^T$  the vector of nodal displacements of a FE, the relationship writes:

$$[U, V, W]^T = \mathbf{D} [u_1, v_1, u_2, v_2, u_3, v_3, u_4, v_4]^T, \quad (20)$$

$\mathbf{D}$  is a interpolation matrix.

It is noted that the discrete displacement at the center of the grain ( $\mathbf{U}$ ) is equal to the finite displacement interpolated in the

**Table 2**  
Reduction in computation time and in DoFs; discrete and continuous models.

	Number of nodes	Number of DoFs	Computation time
Discrete model	625	$625 \times 3 = \mathbf{1875}$	322 s
Continuous model	72	$72 \times 2 = \mathbf{144}$	35 s

center of the grain ( $\mathbf{u}(\mathbf{x})$ ) :  $\mathbf{U} = \mathbf{u}(\mathbf{x})$ . The discrete rotation is also in relation with the finite displacement by:  $\mathbf{W} = \frac{1}{2} (\mathbf{grad} \mathbf{u}(\mathbf{x}) - \mathbf{grad}^T \mathbf{u}(\mathbf{x}))$  in which  $\mathbf{x}$  is the vector position of the grain center's.

At the same time, each DE located at the edge of the discrete zone ( $B^D$ ) is connected to an interpolated DE located at the edge of the continuum zone ( $B^C$ ) by adding half of the interaction energy (19) to the total elastic energy.

Thus, from these two relationships, a DE located in the discrete zone is linked to a FE in the continuum zone. If we use (20) for the interpolated DE ( $\mathbf{U}^-$  or  $\mathbf{U}^+$ ), then the interaction energy (19) between the DE and the FE will be a quadratic function of  $\mathbf{U}^D$  and  $\mathbf{U}^C$ .

$\mathbf{U}^D$  and  $\mathbf{U}^C$  are the global displacements vector of the discrete and continuum zones respectively. By designing  $\mathbf{K}^D$  and  $\mathbf{K}^C$ , the discrete and continuum stiffness matrices, the total energy of the medium will be:

$$\mathbf{E}^{\text{total}} = \frac{1}{2} \begin{pmatrix} \mathbf{U}^C \\ \mathbf{U}^D \end{pmatrix}^T \underbrace{\left[ \begin{pmatrix} \mathbf{K}^C & 0 \\ 0 & \mathbf{K}^D \end{pmatrix} + (\mathbf{K}^{C-D}) \right]}_{\mathbf{K}^{\text{total}}} \begin{pmatrix} \mathbf{U}^C \\ \mathbf{U}^D \end{pmatrix}, \quad (21)$$

$\mathbf{K}^{C-D}$  is the global matrix of interaction which is calculated by the summation of all elementary interaction matrices between the discrete and continuous zones.

By applying an external load to the entire domain noted  $\mathbf{F}$  and using the global stiffness matrix  $\mathbf{K}^{\text{total}}$  calculated in (21), we can find the global displacement vector  $\mathbf{F}$  of the domain by solving the following linear system:

$$\mathbf{K}^{\text{total}} \mathbf{U} = \mathbf{F}. \quad (22)$$

#### 4.2.2. Criterion of coupling

Such as for the 1D methodology (see Hammoud et al., 2010), a criterion of coupling is developed to limit the size of the discrete zone used in the singular zone. The idea is to apply discrete external forces and moments on the DE located at the edge of a FE near the interface zone and to compare the discrete responses of the grains inside the FE to their interpolated FE responses.

The external loading is computed as follows: Using (20), the displacements at the center of the interpolated DE created in the FE can be calculated. From the interaction energy formulated in (19), we calculate the interaction forces and moments between these two DEs using the relation ( $\mathbf{F} = [\mathbf{K}^{\text{interface}}] \cdot [\mathbf{U}^+, \mathbf{U}^-]^T$ ). All the interaction forces between a DE ( $\bullet$ ) and an external interpolated DE ( $\circ$ ) at the edge of FE are computed and assembled to form the external global load applied on the discrete zone included in the FE.

Using the discrete model, we calculate the discrete displacements of the DE noted as  $\mathbf{U}_a^d$ . After that, we calculate the difference between the interpolated continuum displacements in (20),  $\mathbf{U}_i^c$  at the center of grains and  $\mathbf{U}_a^d$ . This difference will be the criterion for coupling. It is formulated as follows:

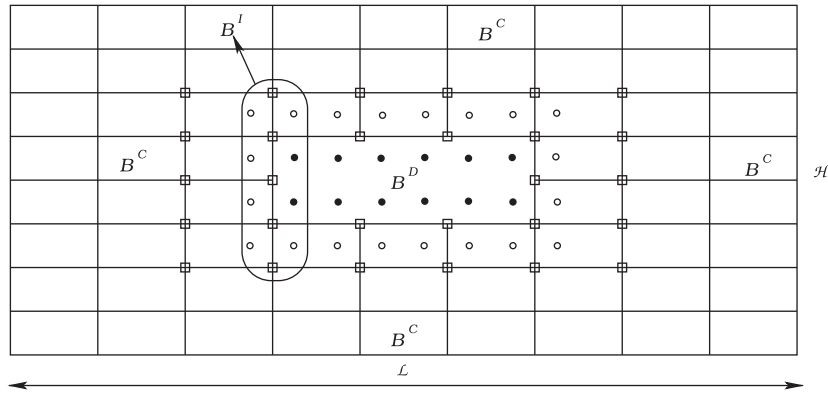


Fig. 7. Regular lattice of square grains modeled by a coupling discrete/continuum model; (●) are the DE of the region ( $B^D$ ), (○) are the interpolated DE of the ( $B^I$ ) and (□) are the finite element nodes of the region ( $B^C$ ).

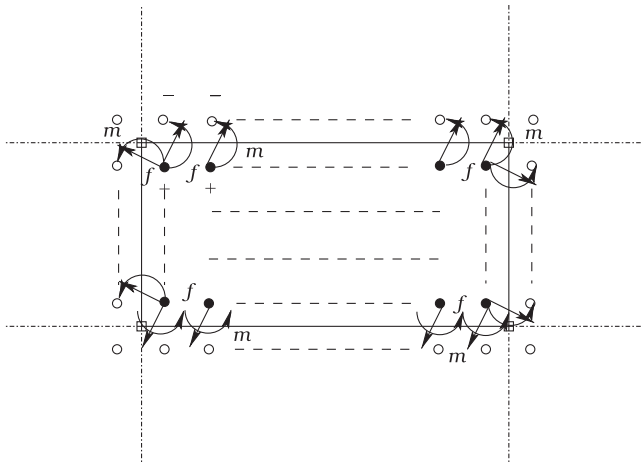


Fig. 8. ( $f, m$ ) are the forces and the moments of interaction between DEs inside the considered FE (●) and interpolated DEs (○) inside adjacent FEs.

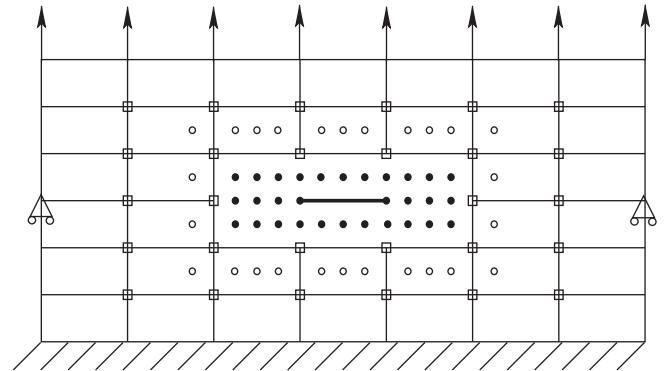


Fig. 10. Masonry panel (width  $L$  and height  $H$ ) subject to traction actions, fixed at the base and simply supported at its left and right edges  $u_1(Y=H/2, X=0) = u_1(Y=H/2, X=L)$ , loaded with a vertical uniform force applied on the bottom; (●) are the DE of the discrete zone, (○) are the interpolated DE at the interface and (□) are the finite element nodes of the continuum zone.

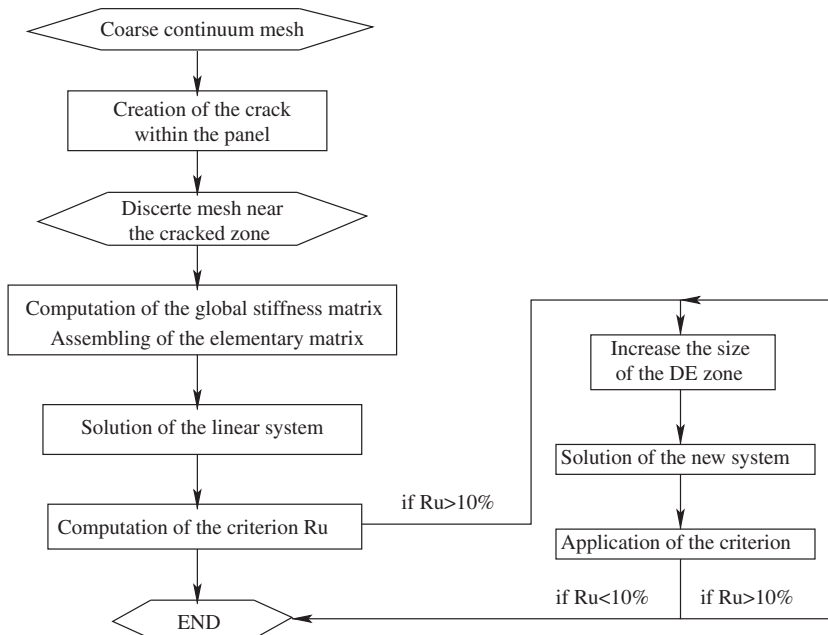


Fig. 9. Numerical algorithm of the coupling model.

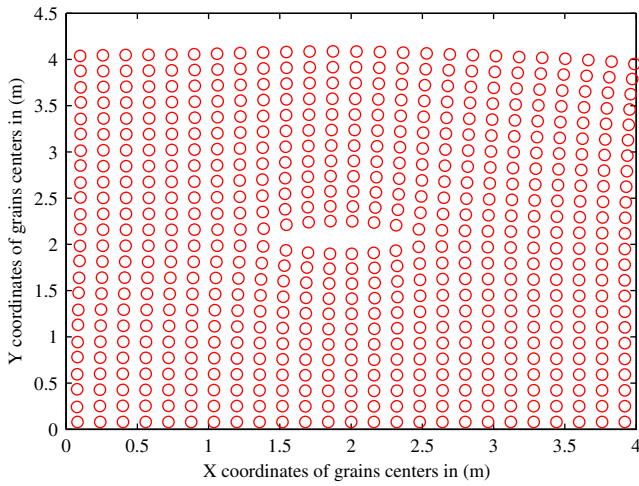


Fig. 11. Discrete simulation of the crack in the panel.

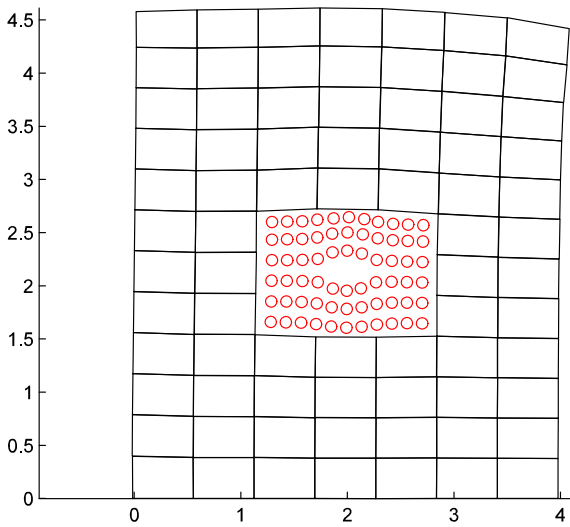


Fig. 12. Coupled simulation of the crack in the panel.

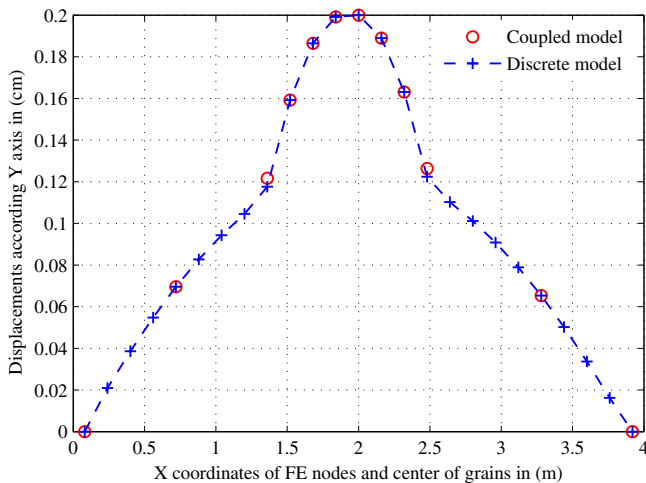


Fig. 13. Comparison between discrete and coupled displacements of the middle line ( $Y = H/2$ ); traction test.

$$R_u = \left| \frac{\mathbf{U}_a^d - \mathbf{U}_i^c}{\mathbf{U}_a^d} \right| \quad (23)$$

By noting “TEST ZONE” the FE zone neighbouring the discrete one, we check the criterion (23) on each FE of this zone. In other words, we check if the FE solution of the “TEST ZONE” coincide with the correct one (i.e the full discrete solution). So if  $R_u$  (23) is not small enough, the size of the discrete zone will be increased. Otherwise, ( $R_u$  is small enough), the size of the discrete zone is then adequate. Thanks to this criterion, the size of the discrete region is limited, and the total number of DoFs is reduced.

4.2.3. Numerical algorithm

At first, the medium is meshed at a coarse scale by using FE. At the center of the medium, a crack is created by broking the interaction between interfaces. The cracked zone is modeled by DE. The size of the discrete zone is fixed. After applying a traction load, for example, we simulate the response of the medium. At the interface between the discrete zone and the continuum one, we check the criterion of coupling described before. Hereafter, a diagram of this algorithm is presented, Fig. 9.

4.2.4. Cracked wall: discrete model vs coupled model

We consider a panel (width  $L=4m$ , height  $H=4m$ ) with a crack at its center. The cracked zone is modeled by DE and the rest of the panel is modeled by FE as shown in Fig. 10.

Firstly a complete discrete simulation is done in order to compare the coupled solution to that discrete. Let us consider a panel modeled by  $25 \times 25$  grains. After a traction load ( $F = 1N$ , we can observe the crack, by simply representing the position of the center of each grain. We can observe in Fig. 11 the rotation of grains considered like rigid bodies.

In this discrete simulation, the number of DoFs is  $625 \times 3$  and the computation time is estimated to 322 s.

Now, let us consider the coupled simulation. The size of a FE is supposed equal to 8 times the size of a DE. The size of the discrete zone is fixed to  $3 \times 3$  FEs which means 72 DEs. The mesh after loading takes the shape seen in Fig. 12.

If we compare the Y displacements of the middle line of the panel, we can observe a perfect match between the discrete and coupled solutions. This agreement is illustrated in Fig. 13.

4.2.5. Gain in time and DoFs

In this paragraph, we underline the advantage of this coupled approach. In the coupled simulation done before, by considering the same dimensions of the panel ( $4 \times 4 m^2$ ), the total number of DoFs is the sum of ( $72 \times 3$  discrete DoFs) and ( $85 \times 2$  continuous DoFs). The computation time is estimated to 54 s. By a simple comparison (see Table 3) between discrete and coupled parameters, we can concluded their importance.

The gain in DoFs is evaluated to:  $G_{DoFs} = \frac{1875}{386} = 4.86$  and the gain in computation time is:  $G_{time} = \frac{322}{54} = 5.96$ . These gain factors will be more interesting in 3D simulations.

By applying the numerical criterion at the interface between discrete and continuum zones, the difference between discrete and continuum solutions is evaluated to 9%. This difference can

Table 3  
Reduction in computation time and in DoFs; coupled and discrete models.

	Number of nodes	Number of DoFs	Computation time
Discrete model	625 DEs	$625 \times 3 = 1875$	322 s
Coupled model	85 FEs + 72 DEs	$85 \times 2 + 72 \times 3 = 386$	54 s

be minimised if we increase the size of the discrete zone. Thus, the gain in DoFs and computation time will decrease.

## 5. Conclusion

In this work a 2D coupled model between discrete and continuum media has been performed. The discrete model is based on interaction between rigid bodies by their interfaces. The continuous model is based on the homogenization of the discrete model. Numerical simulations show that the discrete medium is homogenizable if there is no singularities in the medium. Thus, the continuous model can replace correctly the discrete one. When the medium represents some singularities, a coupled model will be developed. The discrete zone is used to simulate the singularities and elsewhere the continuum zone is used. At the coupling interface, a criterion of coupling is developed. With this criterion, we check if the FEs of the interface leads to the full discrete solution. Another contribution of this coupled method is the sensible gain in terms of DoFs and computation time. The results show a perfect match between the full discrete and coupled discrete/continuous solutions. Thus, it would be more interesting to see the impact of this method on a large structure in 3D simulations. In future works, a code with the ability of remeshing many singularities can be generated. We can study the propagation of many cracks considered in discrete zones. It is also interesting to study the dynamic case and the possibility of spurious reflections at the interface of coupling.

## References

- Alpa, G., Monetto, I., 1994. Microstructural model for dry block masonry walls with in-plane loading. *J. Mech. Phys. Solids* 47 (7), 1159–1175.
- Broughton, J.Q., Abraham, F.F., Bernstein, N., Kaxiras, E., 1999. Concurrent coupling of length scales: methodology and application. *Phys. Rev. B* 60, 2391–2403.
- Cecchi, A., Sab, K., 2009. Discrete and continuous models for in plane loaded random elastic brickwork. *Eur. J. Mech. – A/Solids* 28, 610–625.
- Cecchi, A., Sab, K., 2004. A comparison between 3D discrete and two homogenised plate models for periodic elastic brickwork. *Int. J. Solids Struct.* (9–10), 2259–227.
- Cecchi, A., Sab, K., 2002a. A multi-parameter homogenization study for modelling elastic masonry. *Eur. J. Mech. A/Solids* 21, 249–268.
- Cluni, F., Gusella, V., 2004. Homogenization of non-periodic masonry structures. *Int. J. Solids Struct.* (7), 1911–192.
- Curtin, W.A., Miller, R.A., 2003. Atomistic/continuum coupling in computational materials science. *Modell. Simul. Mater. Sci. Eng.* 11, R33–R68.
- Fish, J., Chen, W., 2004. Discrete-to-continuum bridging based on multigrid principles. *Comput. Methods Appl. Mech. Eng.* 193 (17–20), 1693–1711.
- Florence, C., Sab, K., 2006. A rigorous homogenization method for the determination of the overall ultimate strength of periodic discrete media and an application to general hexagonal lattices of beams. *Eur. J. Mech. A/Solids* (1), 72–9.
- Hammoud, M., Duhamel, D., Sab, K., 2010. Static and dynamic studies for coupling discrete and continuum media; Application to a simple railway track model. *Int. J. Solids Struct.* 47, 276–290.
- Klein, P.A., Zimmerman, J.A., 2006. Coupled atomistic-continuum simulations using arbitrary overlapping domains. *J. Comput. Phys.* 213, 86–116.
- Kohlhoff, S., Gumbsch, P., Fischmeister, H.F., 1991. Crack propagation in bcc crystals studied with a combined finite-element and atomistic model. *Phil. Mag. A* 64 (4), 851–878.
- Pradel, F., Sab, K., 1998a. Homogenization of discrete media. *J. Phys. IV* 8 (P8), 317–324.
- Pradel, F., Sab, K., 1998b. Cosserat modelling of periodic lattice structures. *C.R. Acad. Sci. Paris II b* 326, 699–704.
- Ricci, L., Nguyen, V.H., Sab, K., Duhamel, D., Schmitt, L., 2005. Dynamic behaviour of ballasted railway tracks: a discrete/continuous approach. *Comput. Struct.* 83 (28–30), 2282–2292.
- Rousseau, J., Frangin, E., Marin, P., Daudeville, L., 2008. Damage prediction in the vicinity of an impact on a concrete structure: a combined FEM/DEM approach. *Comput. Concrete* 5 (4), 343–358.
- Rousseau, J., Frangin, E., Marin, P., Daudeville, L., 2009. Multidomain finite and discrete element method for impact analysis of a concrete structure. *Eng. Struct.* 31 (11), 2735–2743.
- Sab, K., 1996. Microscopic and macroscopic strains in a dense collection of rigid particles. *C.R. Acad. Sci. Sér. II Fasc. B - Mécanique Physique Chimie Astronomie* 322 (10), 715–721.
- Wagner, G.J., Liu, W.K., 2003. Coupling of atomistic and continuum simulations using a bridging scale decomposition. *J. Comput. Phys.* 190, 249–274.
- Xiao, S.P., Belytschko, T., 2004. A bridging domain method for coupling continua with molecular dynamics. *Comput. Methods Appl. Mech. Eng.* 193, 1645–1669.